

# Sol–Gel Derived Transparent Zirconium-Phenyl Siloxane Hybrid for Robust High Refractive Index LED Encapsulant

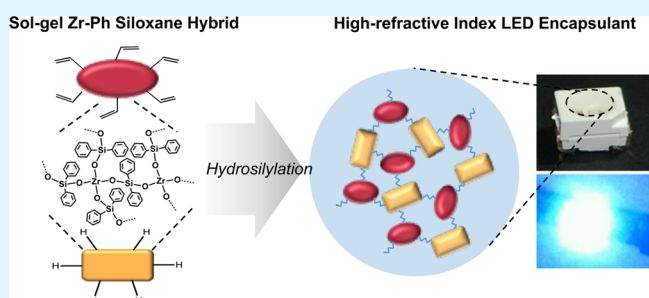
Yong Ho Kim, Jun-Young Bae, Jungho Jin,\* and Byeong-Soo Bae\*

Laboratory of Optical Materials and Coating (LOMC) Department of Materials Science and Engineering, Korea Advanced Institute of Science and Technology (KAIST), Daejeon, Republic of Korea

## S Supporting Information

**ABSTRACT:** We report a zirconium-phenyl siloxane hybrid material (ZPH) that can be used as a robust LED encapsulant. The ZPH encapsulant was fabricated via hydrosilylation-curing of sol–gel derived multifunctional (vinyl- and hydride-functions) siloxane resins containing phenyl-groups and Zr–O–Si heterometallic phase for achieving a high refractive index ( $n \approx 1.58$ ). In thermal aging, the ZPH LED encapsulant exhibited superior performances with a high optical transparency ( $\sim 88\%$  at 450 nm) and exhibited high thermal stability (no yellowing at 180 °C for 1008 h), compared to a commercial LED encapsulant (OE-6630, Dow Corning Corporation). This suggests potential for ZPH to be a robust LED encapsulant.

**KEYWORDS:** LED encapsulant, zirconium oligosiloxane, thermal stability, hybrid material, packaging, optical applications



## INTRODUCTION

Light-emitting diode (LED) is a solid-state lighting device with great potential and currently under intense studies due to its promising traits that are not achievable with conventional light sources such as incandescent bulbs and fluorescent lamps. The most outstanding features of LED include high efficiency coupled with a long lifetime and the use of eco-friendly materials.<sup>1–4</sup> In general, LED as a lighting device is assembled with a LED chip packaged on a reflector cup with wires and heat sinks, which is then encased in an encapsulant containing phosphors. Among these components, the encapsulant plays a critical role in providing long-term reliability of LED by protecting the bottom LED chip from external damages (such as humidity, oxygen, and physical stress). The thermal stability of the encapsulant is another important aspect that needs to be considered in relation to the long-term reliability as the LED junction temperature reaches around 120 °C due to the Joule heating during operation.<sup>5,6</sup> The encapsulant also affects the overall light extraction efficiency of LED. Without an encapsulant, it has been reported that about 75% of emitted light is reflected back to the LED chip by a total internal reflection caused by the difference of refractive indexes between the LED chip ( $n \approx 2.4$  for GaN LED) and air ( $n \approx 1.0$ ).<sup>7</sup> On the basis of the aforementioned considerations, a LED encapsulant should have (i) a high refractive index for improving light extraction from LED chip, and (ii) a sufficiently high thermal stability without any discoloration during a long-term operation of LED.

The materials conventionally used for LED encapsulants are thermosetting epoxy resins and silicone-based materials.<sup>8,9</sup> Despite excellent optical transparency in the visible range and

low gas permeability, thermosetting epoxy resins generally have low refractive index and, more importantly, they cannot maintain their transparency at the operating temperature of LED and undergo heat-induced yellowing.<sup>10</sup> As an attempt to achieve high refractive index, epoxy composite resins in which high refractive index nanoparticles (e.g., ZrO<sub>2</sub>) are dispersed have been reported. However, such epoxy composite resins show degraded thermal stabilities and optical properties due to the lack of particle–matrix interfacial interactions and disturbed cross-linking of the epoxy matrix.<sup>4,11</sup> To address this issue, silicone encapsulants are used as a LED encapsulant due to their excellent thermal stability and optical clarity.<sup>12</sup> For example, methyl-silicone based encapsulants are reported to exhibit excellent optical transparency and high thermal stability. However, methyl-silicone encapsulants in general have low refractive index ( $n \approx 1.4$ ) leading to limited light extraction efficiency. Recently, phenyl-functionalized high refractive index silicone encapsulants are reported.<sup>13,14</sup> We have previously reported a high refractive index phenyl-silicone ( $n \approx 1.578$ ) with high thermal stability.<sup>14</sup>

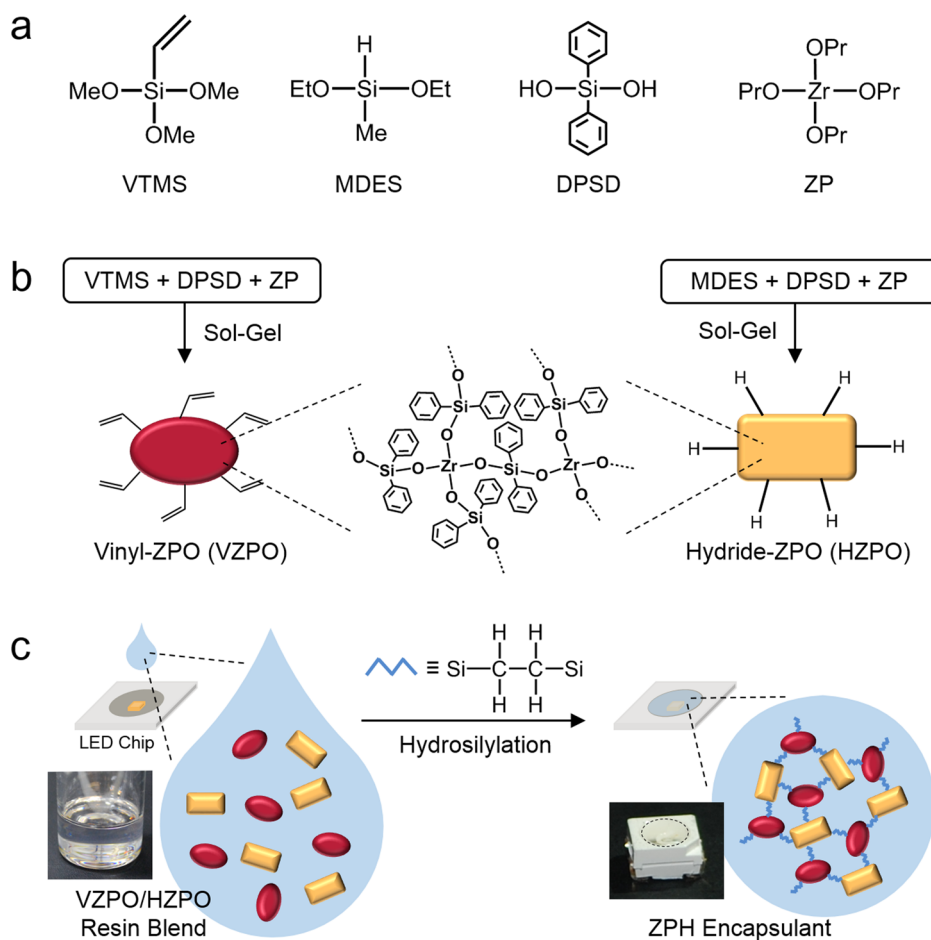
Building on these efforts, in this paper, we report on a high refractive index ( $n \approx 1.58$ ) LED encapsulant based on zirconium-phenyl siloxane hybrid materials (ZPH) exhibiting excellent long-term performance reliability (stable for 1008 h at 180 and 85 °C/85 RH condition). In the ZPH, homogeneous Zr–O–Si heterometallic phases are introduced, along with phenyl groups that have high molecular refractivity, in order for

**Received:** January 16, 2014

**Accepted:** February 21, 2014

**Published:** February 24, 2014

**Scheme 1. Fabrication of Zirconium-Phenyl Siloxane Hybrid (ZPH) for LED Encapsulant:** (a) Chemical Structures of the Precursors Used for Synthesizing VZPO and HZPO Resin; (b) Schematic Illustration of the Synthesis of VZPO and HZPO Resin; VZPO and HZPO are Multifunctional Oligosiloxanes Containing Zr–O–Si Heterometallic Phase That Are Functionalized with Vinyl and Hydride Groups, respectively; (c) Hydrosilylation-Derived Curing of VZPO/HZPO Resin Blend to Fabricate the ZPH Encapsulant; Inset Photographs are the VZPO/HZPO Resin Blend (left) and the ZPH-Encapsulated LED Chip (right)



the final product to achieve a high refractive index of the final product. The homogeneous Zr–O–Si heterometallic phases are introduced via a mild sol–gel condensation, which allows simple preparation of hybrid material.<sup>15</sup>

## RESULTS AND DISCUSSION

As illustrated in Scheme 1, ZPH is fabricated by hydrosilylation-derived curing of a resin blend consisting of vinyl-functionalized zirconium-phenyl oligosiloxane resins (VZPO) and hydride-functionalized zirconium-phenyl oligosiloxane resins (HZPO). Each resin is synthesized via a mild nonhydrolytic sol–gel condensation of diphenylsilanediol (DPSD) and vinyltrimethoxysilane (VTMS) (for VZPO) or methyltriethoxysilane (MDES) (for HZPO) (Scheme 1a, b). For the incorporation of the Zr–O–Si heterometallic phase (Scheme 1b), zirconium *n*-propoxide (ZP) is added dropwise into each resin during the sol–gel synthesis to achieve the formation of the homogeneous heterometallic phase without any precipitation. Otherwise, either the premixing or one-pot addition of the zirconium alkoxide with other silane precursors results in the catastrophic precipitation of zirconium oxides because of the high reactivity of zirconium *n*-propoxide (see the Supporting Information, Figure S1). The synthesized resins (both VZPO and HZPO)

and their resin blend are transparent, colorless and stable. The stability of the resin results from the absence of alkoxy groups (–OR) or hydroxyl groups (–OH) that are potentially reactive sites that may degrade the stability of the resin (see the Supporting Information, Figure S2). The VZPO/HZPO resin blend is then dispensed on a LED chip and subsequently cured via hydrosilylation reaction to form transparent ZPH encapsulant (Scheme 1c).

The molecular structures of both VZPO and HZPO resins were checked by <sup>29</sup>Si NMR and FT-IR (Figure 1). Figure 1a and 1b, respectively, show the <sup>29</sup>Si NMR spectra of VZPO (Zr 3 at%) and HZPO (Zr 3 at%); data from each resin with Zr 1 at% and Zr 5 at% can be found in Figure S3 in the Supporting Information. The <sup>29</sup>Si NMR spectra for both resins confirm the formation of siloxane network (Figure 1a, b), as evidenced by the existence of highly condensed Si species. The different structural environments of the Si atoms can be identified through the chemical shifts of Si (see the inset schemes in Figure 1a, b). VTMS is a trimeric species that is denoted as T<sup>*n*</sup>, where the superscript “*n*” represents the number of siloxanes bound on a Si atom. MDES and DPSD are dimeric species denoted as D<sup>*n*</sup> and D<sup>*n*</sup>, respectively. The degree of

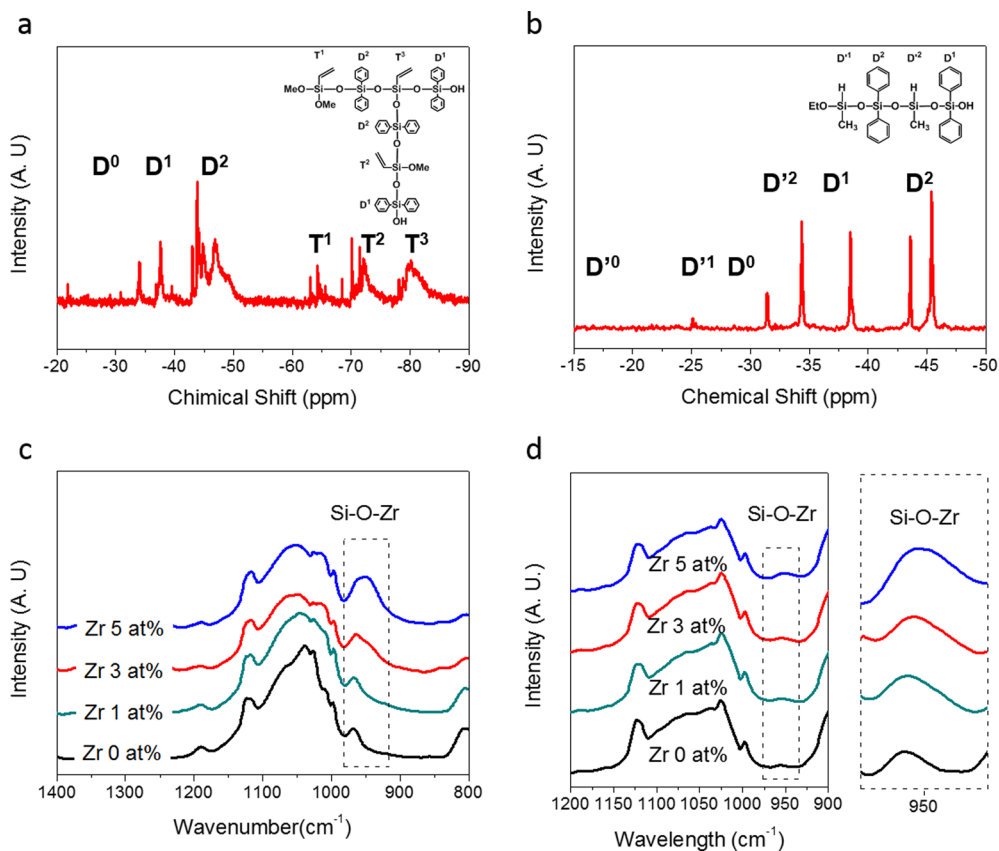


**Figure 1.**  $^{29}\text{Si}$  NMR spectra of (a) VZPO with Zr 3 at %, and (b) HZPO with Zr 3 at %. The inset schemes represent the related structural environment of Si atoms in each resin. FT-IR spectra of (c) VZPO resin and (d) HZPO resin with varying Zr contents. The broad peak at  $1200\text{--}1000\text{ cm}^{-1}$  is assigned to the siloxane network (Si–O–Si), and the broad peak around  $950\text{ cm}^{-1}$  is the signature of the Zr–O–Si heterometallic phases.

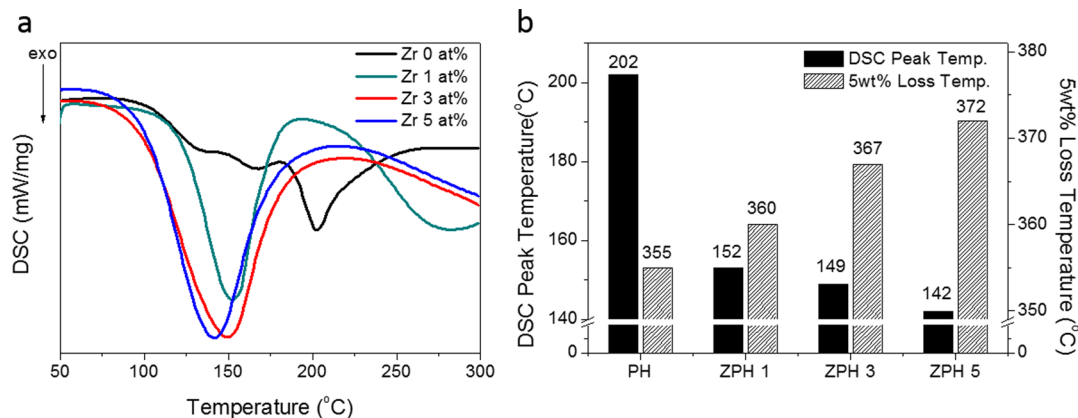


**Figure 2.** Hydro-silylation-curing behaviors of the VZPO/HZPO resin blends and thermal properties of cured ZPH encapsulants. (a) DSC profiles of the VZPO/HZPO resin blends with varying Zr contents. The DSC exothermic peaks are signatures of the hydrosilylation-curing reaction. Note that the introduction of Zr–O–Si phase facilitates the curing reactions, resulting in lower the maximum DSC exothermic peak temperature. (b) The maximum DSC exothermic peak temperatures and 5 wt % loss temperature of the ZPH encapsulants with varying Zr contents (determined from TGA). Note that ZPH exhibits higher thermal stabilities as a result of the facilitated hydrosilylation curing reactions.

condensation (DOC) for the siloxane network is calculated by the following equation:<sup>16</sup>

$$\text{degree of condensation (DOC)} = \frac{D^1 + 2D^2 + T^1 + 2T^2 + 3T^3}{2(D^0 + D^1 + D^2) + 3(T^0 + T^1 + T^2 + T^3)} \times 100$$

The calculated DOC values for VZPO and HZPO with Zr 3 at % were 83.2 and 82.9%, respectively, indicating that the siloxane network is well-formed. The  $^{29}\text{Si}$  NMR spectra show that there are no  $T^0$  and  $D^0$  species, confirming there is no unreacted trimeric and dimeric species of VTMS, MDES, or DPSD.

The existence of Zr–O–Si phase in both VZPO and HZPO resins is checked by FT-IR analysis (Figure 1c, d). In both

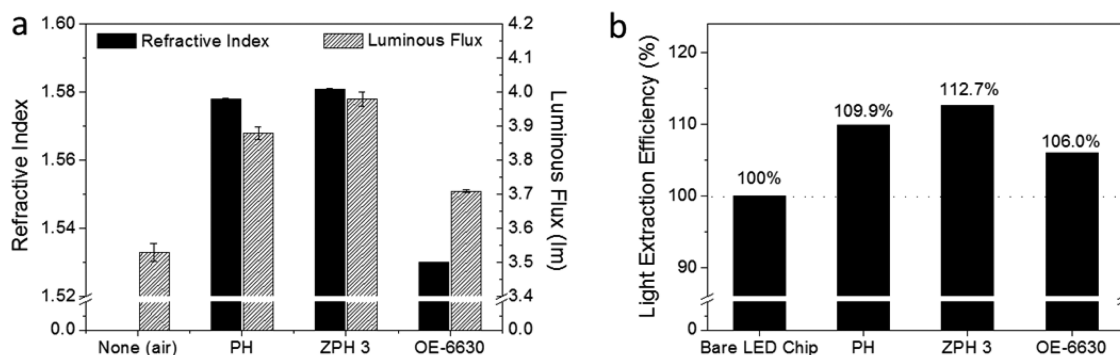


**Figure 3.** Effects of encapsulant's refractive index on light extraction efficiency. (a) Refractive index and corresponding luminous flux values of encapsulated LED chips. A bare LED chip without encapsulant is used as reference. (b) Light extraction efficiency (LEE) of LED chips encapsulated with PH, ZPH3, and OE-6630. The LEE values are normalized with respect to bare LED chip. Note that even a small increase in the encapsulant's refractive index results in noticeable enhancement of LEE.

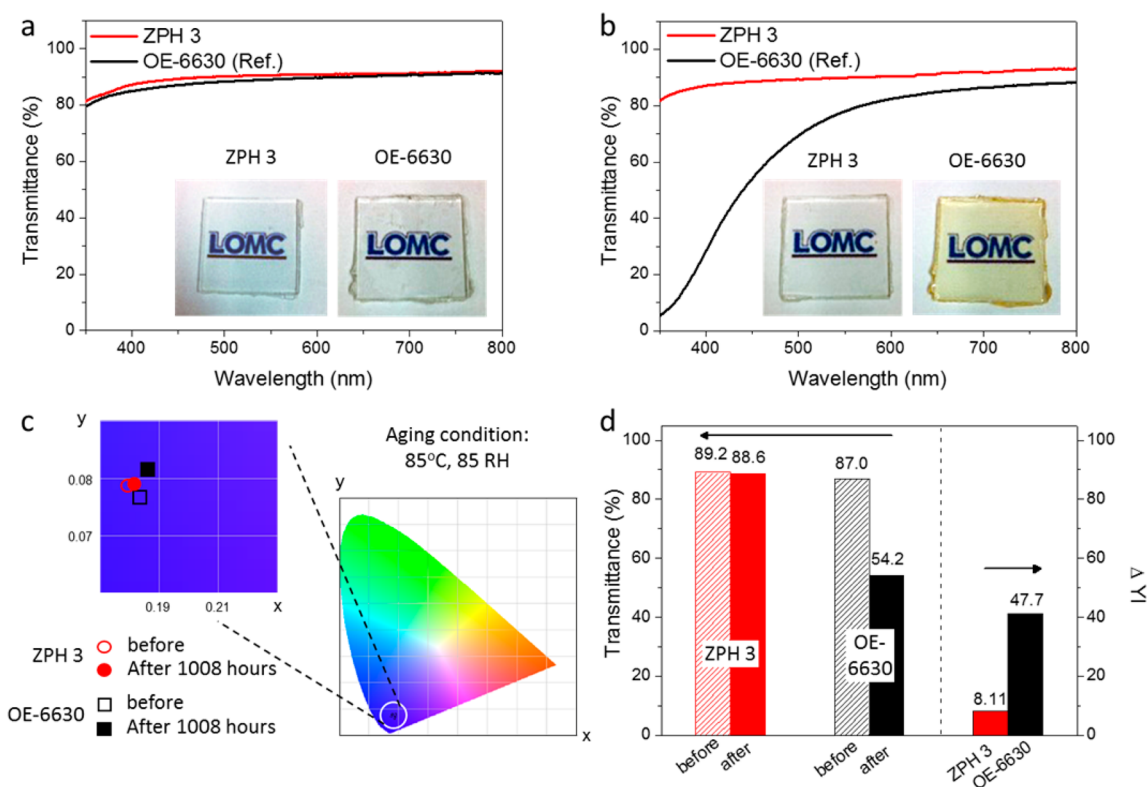


**Figure 4.** Thermal stability tests of ZPH 3 and OE-6630. (a, b) UV-vis spectra of ZPH 3 and OE-6630 bulk sample ( $2 \times 2 \times 0.2 \text{ cm}^3$ ) before and after thermal aging at  $180^\circ\text{C}$  for 1008 h, respectively. (c) CIE color coordinates of the LED encapsulated with ZPH 3 and OE-6630 before and after aging at  $85^\circ\text{C}/85 \text{ RH}$  condition. (d) The change of transmittance (@450 nm) of ZPH 3 and OE-6630 after the thermal aging and change of yellowness index ( $\Delta\text{YI}$ ) of ZPH 3 and OE-6630 encapsulated LED after aging in a thermo-hygrostat at  $85^\circ\text{C}$  and  $85 \text{ RH}$  condition for 1008 h.

spectra, the broad band at  $1000\text{--}1200 \text{ cm}^{-1}$  assigned to the siloxane network (Si–O–Si) is shown, which supports the results from the  $^{29}\text{Si}$  NMR analyses. Note that the peak at  $950 \text{ cm}^{-1}$  in both FT-IR spectra confirms the formation of the Zr–O–Si heterometallic phase, and the intensity of the peak is increased with Zr content.<sup>17–19</sup>

As illustrated in Scheme 1c, the ZPH encapsulant is fabricated by hydrosilylation-derived curing of the VZPO/HZPO resin blend. All the encapsulant samples are designated as ZPH X (X = 1, 3, and 5), where X represents the Zr content from VZPO/HZPO resin blends. For the preparation of the resin blend, VZPO and HZPO resins are mixed in an equivalent ratio of vinyl and hydride groups, which are then compounded

with 80 ppm of platinum catalyst for the hydrosilylation reaction. The hydrosilylation reaction behaviors for the VZPO/HZPO resin blend with varying Zr contents were monitored by DSC (Figure 2a). Interestingly, even with the same amount of catalyst, the VZPO/HZPO resin blend showed a higher reactivity than its zirconium-free version (i.e., vinyl-phenyl oligosiloxane (VPO) and hydride-phenyl oligosiloxane (HPO) resin blend), as evidenced by the lower temperature at the maximum exothermic peak and the larger peak area (Figure 2a, b). This result suggests that the incorporation of zirconium promotes the hydrosilylation reaction. This is thought of as being due to the additional catalytic effect provided by the Zr-containing heterometallic phase, given that the hydrosilylation



reaction is catalyzed not only by late-transition metals like platinum, palladium, and cobalt complexes (Chalk-Harrod mechanism<sup>20</sup>), but also by some early-transition metals such as zirconium and titanium derivatives.<sup>21–24</sup> This additional catalytic effect found in the ZPH is further confirmed in the TGA analysis (Figure 2b and Figure S4 in the Supporting Information). Note that all the ZPH exhibit higher thermal decomposition temperatures compared to the PH (i.e., zirconium-free version), which confirms a higher degree of curing of the ZPH.

The refractive index of ZPH with varying Zr contents and their optical transmittances were assessed by a prism coupler and UV–vis spectrometer, respectively (see Figure S5 in the Supporting Information). As expected, the refractive index of the ZPH increased proportionally with Zr contents due to the high molecular refractivity of the zirconium heterometallic phases.<sup>25</sup> For examining the performance of ZPH as a LED encapsulant, ZPH 3 was selected as the optimal sample as ZPH 3 exhibits best performances in terms of both high refractive index and the initial optical transparency.

The effect that the refractive index of ZPH 3 encapsulant has on the LED light extraction efficiency (LEE) is examined from multiple photoluminescence measurements of the encapsulated LED chips (Figure 3). The LEE,  $\eta_{\text{ext}}$ , is defined by the luminous flux at the observation surface over the total luminous flux from LED chip as follows:<sup>26</sup>

$$\text{light extraction efficiency, } \eta_{\text{ext}} = \frac{\eta_{\text{flux}}}{\eta_{\text{total flux}}}$$

where  $\eta_{\text{flux}}$  is the luminous flux received from observation surface and  $\eta_{\text{total flux}}$  is the total luminous flux generated by the active region of LED. Figure 3a compares the luminous flux values of a bare LED chip and those from LED chips encapsulated with PH, ZPH 3, and OE-6630 (a commercial LED encapsulant from Dow Corning Corporation) along with their refractive index; these values are averaged from multiple measurements. Note that even small increments in the encapsulant's refractive index result in noticeable enhancement in the luminous flux. The normalized LEE values derived from the above equation verify that the LEE can be increased by 12.7% with ZPH 3 encapsulation (Figure 3b).

To evaluate the performance reliability in terms of thermal stability, we annealed the ZPH 3 encapsulant at 180 °C for 1008 h and the transmittance of the ZPH 3 was checked before (Figure 4a) and after (Figure 4b) the thermal aging. The OE-6630 encapsulant was used as reference for comparison. For the ZPH 3, the transmittance value (88% at 450 nm) was maintained even after 1008 h of aging without any discoloration (photographs shown in the inset of Figures 4a and 4b), while OE-6630 ended up with a considerable degradation in the transmittance. This result confirms the excellent long-term high-thermal stability of the ZPH 3 encapsulant. The long-term reliability of the ZPH 3 encapsulant was further checked in an additional test using a thermo-hygrostat, in which the encapsulated LED was aged under 85 °C and 85 RH condition for 1008 h. Then the CIE color coordinates and the luminous flux of the encapsulated LEDs were measured before and after aging (Figure 4c and Figure S6 in the Supporting Information). From the measured CIE color coordinate value of the encapsulated LED, a yellowness index (YI) was calculated by the following equation (ASTM D1945):

$$\text{yellowness index (YI)} = 100 \times \frac{1.28X - 1.06Z}{Y}$$

The calculated  $\Delta$ YI value of the ZPH 3 was remarkably smaller than that of OE-6630 (Figure 4d), and the variation of luminous flux value of the ZPH 3 encapsulated LED was also smaller than that OE-6630 (see the Supporting Information, Figure S6), which shows a consistent tendency as in the case of thermal aging.

Thermomechanical property, which is important for LED encapsulant, of the ZPH 3 was confirmed by dynamic mechanical analysis (DMA) in the temperature range from –50 to 200 °C. The rubbery state storage modulus is about 70 MPa, which is comparable to that of OE-6630 (~40 MPa), confirming that the ZPH 3 encapsulant possesses sufficiently workable thermomechanical characteristic as LED encapsulant (see the Supporting Information, Figure S7).

## CONCLUSIONS

In summary, we report a robust, high refractive index ( $n \approx 1.58$ ) LED encapsulant using zirconium-phenyl siloxane hybrid material (ZPH). The ZPH was fabricated via hydrosilylation between the sol–gel derived vinyl- and hydride- functionalized zirconium-phenyl oligosiloxanes, containing Zr–O–Si heterometallic phases. The Zr–O–Si heterometallic phase gives not only enhanced refractive index but also an additional catalytic effect to the hydrosilylation reaction. The optical properties of the ZPH maintained after 1008 h of thermal aging at 180 °C, showed excellent thermal resistance against discoloration. These high thermal stability and high refractive index are critical characteristics for the LED encapsulant for long-term reliability of LED.

## EXPERIMENTAL SECTION

**Synthesis of VZPO Resin.** Vinyltrimethoxysilane (VTMS, > 98%, Tokyo Chemical Industry), zirconium n-propoxide (ZP, 70% solution in 1-propanol, Aldrich), and diphenylsilanediol (DPSD, 98%, Gelest) were used as precursors. Barium hydroxide monohydrate (Aldrich) was added as a basic catalyst to promote reaction (0.1 mol % of total silane precursors) and *p*-xylene (Aldrich) were added for homogeneous synthesis (10 wt % of total precursors). We synthesized VZPO resin using nonhydrolytic sol–gel condensation of VTMS and DPSD (1:1 molar ratio) at 80 °C while stirring. After the resin being clear, ZP was added dropwise into the resin (1, 3, and 5 mol % of total Si). A clear, homogeneous resin could not be obtained when the Zr contents is more than 5%. Total reaction time was 4 h. The synthesized resins were filtered through a 0.45  $\mu\text{m}$  Teflon filter and vacuum heated to remove volatile components.

**Synthesis of HZPO Resin.** Methyl-diethoxysilane (MDES, Gelest), ZP, and DPSD were used as precursors. Amberlite IRC76 (Aldrich) was added as an acidic catalyst to promote reaction (0.1g for 0.2 mol of total silane precursors). Because the silicon hydride group is damaged by basic condition, the acidic catalyst was used for sol–gel reaction. We synthesized HZPO resin using nonhydrolytic sol–gel condensation of MDES and DPSD (1:1.5 molar ratio) at 100 °C. After an hour, ZP was added dropwise into the resin (1, 3, and 5 mol % of total Si). A clear, homogeneous resin could not be obtained when the Zr contents is more than 5%. Total reaction time was 12 h. The synthesized resins were filtered through a 0.45  $\mu\text{m}$

Teflon filter and vacuum heated to remove volatile components.

**Fabrication of ZPH.** The VZPO resin was mixed with the HZPO resin in a 1:1 vinyl:hydride ratio and a 0.4 wt % (80 ppm) of Pt Karstedt's catalyst [Platinum(0)-1,3-divinyl-1,1,3,3-tetramethyldisiloxane complex solution in *p*-xylene (~2% Pt), Aldrich] was added. For the thermal hydrosilylation reaction between vinyl groups and hydrosilane groups, the mixed resins were cast into a glass mold (thickness = 2 mm), then heat cured at 150 °C for 3 h in air.

**LED Encapsulation.** The encapsulants were dispensed on LED, and then surface-flattening was followed for consistency of the encapsulating process. The LED encapsulation using ZPH was processed at 150 °C for 3 h in air, which is the same condition for the fabrication of ZPH bulk; the curing temperature was determined from the DSC analysis. The LED encapsulation using PH was carried out at 150 °C for 4 h in air as reported in the previous paper.<sup>14</sup> Finally, the LED encapsulation using OE-6630 was conducted at 150 °C for an hour in air, which is same condition in the catalog from Dow Corning Corporation (See <http://www.dowcorning.com/applications/search/default.aspx?R=6577EN> for more details).

**Characterizations.** The <sup>29</sup>Si nuclear magnetic resonance (NMR) spectra of the VZPO and HZPO resins with chromium acetylacetonate (concentration of 30 mg/L) in 50 vol % chloroform-*d* were measured using a FT 500 MHz (Bruker Biospin, DMX600). Fourier transform-infrared (FT-IR) spectra (JASCO, FTIR 460 plus) were measured in air to confirm the molecular structure of VZPO and HZPO. Differential scanning calorimeter (DSC, Netzsch, DSC 200 F3Maia) curves were measured in air to study the thermal hydrosilylation curing behavior of VZPO/HZPO resin blends with Pt catalyst. A thermal gravimetric analysis (TGA, TA TGA Q50) was performed in air condition to measure thermal decomposition of the ZPH. The optical transmittances the ZPH and OE-6630 bulks were measured by an ultraviolet–visible–near-infrared (UV/vis/NIR) spectrophotometer (Shimadzu, UV-3101PC). Luminous flux and CIE color coordinates of the encapsulated LEDs were measured by a DARSA PRO 5100 PL System (PSI Trading Co., Ltd.) under a forward bias current of 20 mA at room temperature. An integrating sphere was used for the measurement. The refractive index of the ZPH was measured by prism coupler (Metricon, 2010/M) at 633 nm. The dynamic mechanical analysis (DMA, TA 2980 DMA) was performed in the temperature range from –50 to 200 °C with 5 °C/min ramping rate under 1 Hz and 0.15 μm oscillating amplitude.

## ■ ASSOCIATED CONTENT

### 📄 Supporting Information

A photograph of the precipitated resin, FT-IR and <sup>29</sup>Si NMR spectra of VZPO and HZPO resin with varying Zr contents, TGA profiles, refractive index, initial transmittance of ZPH with varying Zr contents, the luminous flux change of encapsulated LED with ZPH 3 and OE-6630 before and after aging in thermo-hygrostat, and dynamic mechanical analysis (DMA) curve of ZPH 3. This material is available free of charge via the Internet at <http://pubs.acs.org/>.

## ■ AUTHOR INFORMATION

### Corresponding Authors

\*E-mail: [jinuine@kaist.ac.kr](mailto:jinuine@kaist.ac.kr).

\*E-mail: [bsbae@kaist.ac.kr](mailto:bsbae@kaist.ac.kr).

## Notes

The authors declare no competing financial interest.

## ■ ACKNOWLEDGMENTS

This work was supported by the National Research Foundation of Korea (NRF) grant funded by the Korea government (MSIP) (NRF-2013R1A2A2A05005911). We gratefully thank to the Korea Basic Science Institute (KBSI) for <sup>29</sup>Si NMR spectra measurement and to Seoul Semiconductor Co. for providing the lead framed LED chips.

## ■ REFERENCES

- (1) Patel, P. Solid-State Lighting: The Future Looks Bright. *MRS Bull.* **2011**, *36*, 678–680.
- (2) Tsami, A.; Yang, X.-H.; Galbrecht, F.; Farrell, T.; Li, H.; Adamczyk, S.; Heiderhoff, R.; Balk, L. J.; Neher, D.; Holder, E. Random Fluorene Copolymers with on-Chain Quinoxaline Acceptor Units. *J. Polym. Sci., Part A: Polym. Chem.* **2007**, *45*, 4773–4785.
- (3) Kanelidis, I.; Ren, Y.; Lesnyak, V.; Gasse, J.-C.; Frahm, R.; Eychmüller, A.; Holder, E. Arylamino-Functionalized Fluorene- and Carbazole-Based Copolymers: Color-Tuning Their CdTe Nanocrystal Composites from Red to White. *J. Polym. Sci., Part A: Polym. Chem.* **2011**, *49*, 392–402.
- (4) Tao, P.; Li, Y.; Siegel, R. W.; Schadler, L. S. Transparent Dispensable High-Refractive Index ZrO<sub>2</sub>/epoxy Nanocomposites for LED Encapsulation. *J. Appl. Polym. Sci.* **2013**, *130*, 3785–3793.
- (5) Narendran, N.; Gu, Y.; Freyssonier, J. P.; Yu, H.; Deng, L. Solid-State Lighting: Failure Analysis of White LEDs. *J. Cryst. Growth* **2004**, *268*, 449–456.
- (6) Narendran, N.; Gu, Y. Life of LED-Based White Light Sources. *J. Disp. Technol.* **2005**, *1*, 167–171.
- (7) Chhajed, S.; Lee, W.; Cho, J.; Schubert, E. F.; Kim, J. K. Strong Light Extraction Enhancement in GaInN Light-Emitting Diodes by Using Self-Organized Nanoscale Patterning of P-Type GaN. *Appl. Phys. Lett.* **2011**, *98*, 071102.
- (8) Hsu, C.-W.; Ma, C.-C. M.; Tan, C.-S.; Li, H.-T.; Huang, S.-C.; Lee, T.-M.; Tai, H. Effect of Thermal Aging on the Optical, Dynamic Mechanical, and Morphological Properties of Phenylmethylsiloxane-Modified Epoxy for Use as an LED Encapsulant. *Mater. Chem. Phys.* **2012**, *134*, 789–796.
- (9) Huang, W.; Zhang, Y.; Yu, Y.; Yuan, Y. Studies on UV-Stable Silicone–epoxy Resins. *J. Appl. Polym. Sci.* **2007**, *104*, 3954–3959.
- (10) Bourget, L.; Corriu, R. J. P.; Leclercq, D.; Mutin, P. H.; Vioux, A. Non-Hydrolytic Sol–gel Routes to Silica. *J. Non. Cryst. Solids* **1998**, *242*, 81–91.
- (11) Chung, P. T.; Yang, C. T.; Wang, S. H.; Chen, C. W.; Chiang, A. S. T.; Liu, C.-Y. ZrO<sub>2</sub>/epoxy Nanocomposite for LED Encapsulation. *Mater. Chem. Phys.* **2012**, *136*, 868–876.
- (12) Katayama, S.; Yamada, N.; Shibata, Y.; Noda, K. Fabrication and Properties of PDMPS-Based Inorganic/organic Hybrid Sheets. *J. Ceram. Soc. Japan* **2003**, *111*, 391.
- (13) Mosley, D. W.; Khanarian, G.; Conner, D. M.; Thorsen, D. L.; Zhang, T.; Wills, M. High Refractive Index Thermally Stable Phenoxyphenyl and Phenylthiophenyl Silicones for Light-Emitting Diode Applications. *J. Appl. Polym. Sci.* **2014**, *131*, 39824.
- (14) Kim, J.-S.; Yang, S. C.; Kwak, S.-Y.; Choi, Y.; Paik, K.-W.; Bae, B.-S. High Performance Encapsulant for Light-Emitting Diodes (LEDs) by a Sol–gel Derived Hydrogen Siloxane Hybrid. *J. Mater. Chem.* **2012**, *22*, 7954.
- (15) Livage, J. Sol–Gel Synthesis of Hybrid Materials. *Bull. Mater. Sci.* **1999**, *22*, 201–205.
- (16) Sepeur, S.; Kunze, N.; Werner, B.; Schmidt, H. UV Curable Hard Coatings on Plastics. *Thin Solid Films* **1999**, *351*, 216–219.
- (17) Kulkarni, S. Sol-Gel Immobilized Cyano-Polydimethylsiloxane and Short Chain Polyethylene Glycol Coatings for Capillary Microextraction Coupled to Gas Chromatography. *University of South Florida* **2007**.

(18) Dang, Z.; Anderson, B. G.; Amenomiya, Y.; Morrow, B. a. Silica-Supported Zirconia. 1. Characterization by Infrared Spectroscopy, Temperature-Programmed Desorption, and X-Ray Diffraction. *J. Phys. Chem.* **1995**, *99*, 14437–14443.

(19) Guerneur, C.; Lambard, J.; Gerard, J.-F.; Sanchez, C. Hybrid Polydimethylsiloxane-Zirconium Oxo Nanocomposites. Part 1 Characterization of the Matrix and the Siloxane-Zirconium Oxo Interface. *J. Mater. Chem.* **1999**, *9*, 769–778.

(20) Chalk, A. J.; Harrod, J. F. Homogeneous Catalysis. II. The Mechanism of the Hydrosilation of Olefins Catalyzed by Group VIII Metal Complexes 1. *J. Am. Chem. Soc.* **1965**, *87*, 16–21.

(21) Harrod, J. F.; Yun, S. S. Silyltitanocene Complexes as Catalysts for the Hydrogenation, Isomerization, and Hydrosilylation of Olefins. *Organometallics* **1987**, *6*, 1381–1387.

(22) Corey, J. Y.; Zhu, X. H. Reactions of Hydrosilanes and Olefins in the Presence of Cp<sub>2</sub>MCl<sub>2</sub>/BuLi. *Organometallics* **1992**, *11*, 672–683.

(23) Van der Linden, A.; Schaverien, C. J.; Meijboom, N.; Ganter, C.; Orpen, A. G. Polymerization of  $\alpha$ -Olefins and Butadiene and Catalytic Cyclotrimerization of 1-Alkynes by a New Class of Group IV Catalysts. Control of Molecular Weight and Polymer Microstructure via Ligand Tuning in Sterically Hindered Chelating Phenoxide Titanium. *J. Am. Chem. Soc.* **1995**, *117*, 3008–3021.

(24) Froese, R. D. J.; Musaev, D. G.; Matsubara, T.; Morokuma, K. Theoretical Studies of Ethylene Polymerization Reactions Catalyzed by Zirconium and Titanium Chelating Alkoxide Complexes. *J. Am. Chem. Soc.* **1997**, *119*, 7190–7196.

(25) Tao, P.; Li, Y.; Rungta, A.; Viswanath, A.; Gao, J.; Benicewicz, B. C.; Siegel, R. W.; Schadler, L. S. TiO<sub>2</sub> Nanocomposites with High Refractive Index and Transparency. *J. Mater. Chem.* **2011**, *21*, 18623.

(26) Chen, X.; Kong, F.; Li, K.; Ding, Q.; Zhang, M.; Li, W. Study of Light Extraction Efficiency of Flip-Chip GaN-Based LEDs with Different Periodic Arrays. *Opt. Commun.* **2014**, *314*, 90–96.